Catalysis Today 151 (2010) 338–346

Contents lists available at ScienceDirect

Catalysis Today

journal homepage: www.elsevier.com/locate/cattod

Effect of ceria on the desulfation characteristics of model lean NO_x trap catalysts

Vencon Easterling [a], Yaying Ji [a], Mark Crocker [a,*], Justin Ura [b], Joseph R. Theis [b], Robert W. McCabe [b]

[a] Center for Applied Energy Research, University of Kentucky, 2540 Research Park Drive, Lexington, KY 40511, United States
[b] Research and Innovation Center, Ford Motor Company, 2101 Village Road, Dearborn, MI 48124, United States

ARTICLE INFO

Article history:
Available online 18 January 2010

Keywords:
Lean NO_x trap
NO_x storage catalyst
Sulfation
Desulfation
Ceria

ABSTRACT

Using model powder catalysts and fully formulated monolithic lean NO_x trap (LNT) catalysts, the effect of ceria on LNT desulfation behavior was investigated. TPR experiments performed on the model catalysts showed that each of the oxide phases present (BaO, CeO_2, and Al_2O_3) is able to store sulfur and that they possess distinct behavior in terms of the temperatures at which desulfation occurs. For a $Pt/BaO/Al_2O_3$ catalyst, addition of ceria was found to reduce the degree of sulfur accumulation on the BaO phase, particularly at high sulfur loadings, by contributing to sulfur capture. The importance of maintaining the Pt and Ba phases in close proximity for efficient LNT desulfation was also demonstrated; physically separating the Pt and Ba sites resulted in a shift of the desulfation temperature of the surface $BaSO_4$ by 20–40 °C towards higher temperature, i.e., towards the position characteristic of bulk $BaSO_4$. From the monolith studies, it was found that relative to a sample containing no ceria, samples containing La-stabilized CeO_2 or CeO_2–ZrO_2 showed a greater resistance to deactivation during sulfation (as reflected by the NO_x storage efficiency), and required lower temperatures to restore the NO_x storage efficiency to its pre-sulfation value. In addition to the ability of ceria to store sulfur and release it at relatively low temperatures under reducing conditions, these findings can be attributed to the high water–gas shift activity displayed Pt/CeO_2, which result in increased intra-catalyst concentrations of H_2 under rich conditions. The results also showed that precious metal loadings can significantly impact desulfation efficiency and that both high Rh and Pt loadings are beneficial for catalyst desulfation.

1. Introduction

Lean-burn engines have the potential to provide better fuel economy than current stoichiometric engines though reduced pumping losses and enhanced combustion thermodynamics [1]. Although reduced CO_2 and hydrocarbon emissions are seen from lean-burn engines, NO_x emissions do not meet current emission standards when these engines are coupled with three-way catalytic converters. This short-coming is caused by the inability of NO_x to be reduced to nitrogen in atmospheres containing excess oxygen. To date, two main solutions have been proposed and implemented. One method is selective catalytic reduction (SCR) where ammonia is used as the reductant to convert NO_x to nitrogen [2]. The other method is the use of lean NO_x traps (LNTs). A LNT catalyst usually consists of a platinum group metal to oxidize the NO to NO_2, an alkali or alkaline earth metal oxide to store NO_x (e.g., BaO), and a high surface area support material (e.g., γ-alumina) [3].

Although LNTs are starting to find commercial application, the issue of LNT durability remains problematic. Sulfur present in fuel and engine oil is converted to SO_2 through the combustion cycle of engine operation, and the SO_2 can subsequently undergo oxidation over precious metals, such as Pt and Rh, to form SO_3. Barium oxide has a greater affinity for SO_3 than NO_2 (the resulting $BaSO_4$ being thermodynamically more stable than $Ba(NO_3)_2$ [4]), resulting in poisoning of the NO_x storage sites. The decomposition of $BaSO_4$ requires the LNT to be exposed to rich conditions and high temperatures (650–800 °C) for several minutes. This requirement results in a fuel penalty that reduces the gains in fuel efficiency of lean-burn engines and gives rise to sintering of the precious metals and NO_x storage components. The high temperatures also enable unwanted side reactions between the LNT washcoat components (e.g., resulting in formation of $BaAl_2O_4$ and $BaCeO_3$) [5–8]. The formation of $BaAl_2O_4$ and $BaCeO_3$ and growth of Pt particles due to sintering decreases LNT NO_x storage efficiency [9–11]. Some researchers have attributed this decrease in efficiency to the reduced spillover rate of NO_2, formed from the oxidation of NO over Pt, to the storage material [5,12,13].

Recent studies have shown that ceria in LNTs is able to store some of the sulfur in the exhaust with the consequence that fewer barium sites should be poisoned [1,14–17]. The use of ceria as a component of three-way catalysts is well established based on its ability to reversibly store oxygen (that acts as a damper in

* Corresponding author. Tel.: +1 859 257 0295; fax: +1 859 257 0302.
E-mail address: crocker@caer.uky.edu (M. Crocker).

0920-5861/$ – see front matter © 2009 Elsevier B.V. All rights reserved.
doi:10.1016/j.cattod.2009.12.007

maintaining stoichiometric conditions during various engine operating ranges) and its ability to maintain high precious metal dispersions in the washcoat [18]. The main function of ceria in lean-burn gasoline LNTs is similarly to act as an oxygen storage material, thereby enabling the LNT to function as a conventional three-way catalyst when the engine is operating under stoichiometric conditions. However, different research groups have reported additional benefits from the incorporation of ceria in LNTs. Theis et al. reported that the addition of ceria improved the sulfur tolerance of the LNT [1]. In addition to improved sulfur tolerance, Kwak et al. reported that ceria-containing catalysts provide excellent resistance against Pt sintering as compared to alumina-based catalysts [16]. Using DRIFTS, Ji et al. showed the addition of ceria improved sulfur resistance by reducing sulfur accumulation on BaO sites [17]. In addition, Ji proposed that the addition of ceria would lower the fuel penalty and precious metal sintering associated with catalyst desulfation because the operating period between desulfation events could be extended. The presence of ceria has also been shown to improve the NO_x storage and reduction properties of LNTs, particularly at low temperatures [19–21]. Furthermore, under rich conditions, Pt promoted ceria is known to catalyze the water–gas shift reaction that produces hydrogen and CO_2 from CO and water [22,23]. The additional hydrogen produced is available to regenerate the trap, which is very beneficial given that H_2 has been shown to be a better NO_x reductant than CO [24–29]; likewise, H_2 is a more efficient reductant for LNT desulfation than CO [29,30].

Although ceria possesses these attractive characteristics when used in LNT catalysts, to date relatively few reports have dealt directly with its role in LNT sulfation and desulfation. In this study the effect of ceria on sulfation and desulfation behavior was investigated, using both model powder catalysts and fully formulated monolithic catalysts. The effect of precious metal loading and the importance of Pt location (relative to the Ba phase) on the ease of LNT desulfation were also examined.

2. Experimental

2.1. Preparation of powder catalyst samples

Powder samples were prepared by incipient wetness impregnation. Pt/Al_2O_3 was made by impregnating γ-alumina (Sasol, surface area of 132 m^2/g) with an aqueous solution of tetraamine-platinum (II) nitrate. The sample was then dried under vacuum at 100 °C overnight and calcined in air at 500 °C for 3 h. Pt/CeO_2 was prepared by the same method using ceria (Rhodia, surface area of 119 m^2/g). A stepwise method was used to make the $Pt/BaO/Al_2O_3$ sample (denoted PBA). γ-Alumina was impregnated with aqueous $Ba(NO_3)_2$, dried and calcined at 500 °C in air. The Ba-loaded Al_2O_3 was then impregnated with aqueous tetraamine-platinum (II) nitrate and again calcined at 500 °C. Finally, in order to investigate the effect of ceria addition on the $Pt/BaO/Al_2O_3$ catalyst, a sample was prepared by physically mixing the $Pt/BaO/Al_2O_3$ and Pt/CeO_2 powders in a 76:24 weight ratio (denoted PBAC). All of the powders were pressed into pellets using an IR pellet press and then crushed and screened to a size of ASTM 20–40 mesh.

2.2. Temperature-programmed sulfation–desulfation experiments

Each of the powder catalysts was subjected to a temperature-programmed reduction (TPR) procedure to determine the temperature required to decompose the sulfates stored on the different storage components. The microreactor used consisted of a 1/4 in. o.d. quartz tube in which a section of ca. 3 in. length contained the 150 mg of powder catalyst. The tube was heated by a programmable Lindberg Blue furnace. A V&F Airsense 2000 chemical ionization mass spectrometer (CI-MS) analyzed the product gases from the reactor. A gas flow rate of 120 sccm was used, corresponding to a gas space velocity of ca. 30,000 h^{-1}. Table 1 shows the lean and rich feed gas compositions for the powder reactor. All of the inlet and outlet lines for the reactor were heated using heat tape to above 100 °C to prevent water condensation prior to analysis in the CI-MS.

Table 1
Feed composition for experiments utilizing powder catalysts.

Component	Pre-oxidation	Pre-reduction	Sulfation	TPR
SO_2	0	0	100 ppm	0
O_2	8%	0	8%	0
H_2	0	2%	0	2%
CO_2	5%	5%	5%	5%
H_2O	5%	5%	5%	5%
Ar	Balance	Balance	Balance	Balance
Total gas flow, sccm	120	120	120	120
GHSV, h^{-1}	30,000	30,000	30,000	30,000

Prior to the experiments, each sample was subjected to pretreatment at 450 °C. The sample was first oxidized in a mixture of 8% O_2, 5% CO_2 and 5% H_2O (with Ar as the balance) for 15 min, after which it was purged with 5% CO_2 and 5% H_2O (with Ar as the balance) for 10 min. The sample was then reduced in 2% H_2, 5% CO_2, 5% H_2O, and balance Ar. Finally, the sample was cooled to 350 °C while it was exposed to 5% CO_2 and 5% H_2O (with Ar as the balance).

The powder samples were sulfated by exposure to a feed containing 100 ppm SO_2, 8% O_2, 5% CO_2, 5% H_2O, and balance Ar (feed rate of 120 sccm) for 34 min at 350 °C. Assuming complete sulfur uptake, these conditions resulted in a loading equivalent to 1 g sulfur/L for a monolithic catalyst with a washcoat loading of 260 g/L. Higher loadings were achieved by extending the duration of the sulfation. The catalysts were then subjected to desulfation under reducing conditions for the TPR. The procedure consisted of exposing the sample to 2% H_2, 5% CO_2 and 5% H_2O (with Ar as the balance) as the temperature was increased from 350 to 800 °C at a rate of 5 °C/min. The product gas stream was analyzed using the CI-MS.

2.3. Preparation of monolith catalyst samples

The samples, listed in Table 2, are categorized into three groups according to the variation in components. The preparation of the catalysts has been described in detail elsewhere [21]. In brief, the samples were prepared using the incipient wetness method. In a first step, Pt and Rh were co-impregnated in a 1:1 weight ratio (using $Pt(NH_3)_4(OH)_2$ and $Rh(NO_3)_3$ as the precursors) onto γ-alumina stabilized with 3 wt.% La_2O_3, after which the powder was calcined for 2 h at 500 °C. Separately, BaO/Al_2O_3 was prepared by

Table 2
Composition of monolith catalysts.

Component	Catalyst code/component loading[a]		
	Series 1	Series 2	Series 3
Pt, g/L (g/cuft)	3.53 (100)	3.53 (100)	3.53 (100), 1.77 (50)
Rh, g/L (g/cuft)	0.71 (20)	0.71 (20)	0.35 (10)
BaO, g/L	30	30	30
CeO_2[b], g/L	0, 50, 100	0	50
CeO_2–ZrO_2[c], g/L	0	50, 100	0
Al_2O_3[d], g/L	Balance	Balance	Balance

[a] Nominal loadings. Total washcoat loading = 260 g/L.
[b] Stabilized with 5 wt.% La_2O_3.
[c] $Ce_{0.7}Zr_{0.3}O_2$.
[d] Stabilized with 3 wt.% La_2O_3.

impregnating $Ba(O_2CCH_3)_2$ onto γ-alumina, followed by calcination (also at 500 °C for 2 h). To this the required amount of CeO_2 or CeO_2–ZrO_2 was added. To achieve the total Pt loading, the balance of the Pt was then impregnated onto the mixture as (as $Pt(NH_3)_4(OH)_2$), after which it was calcined at 500 °C for 2 h. The Pt and Rh containing powder (in an amount corresponding to 30 g/L) and the powder containing BaO/Al_2O_3 and CeO_2 was added to a balance of γ-alumina powder to achieve the overall washcoat loading of 260 g/L. A small amount of boehmite sol was used as a binder. The resulting slurry was washcoated onto a 4 in. × 6 in. cordierite 400 cpsi/6.5 mil monolith by DCL International, Inc. (Toronto, ON) using a proprietary vacuum coating process. The monoliths were calcined at 550 °C for 2 h.

In series 1, the sample codes reflect the amount of barium (held constant at 30 g/L) and the amount of CeO_2 present (0, 50, or 100 g/L). Series 2 is composed of two samples designated 30–50*z* and 30–100*z*. The "*z*" refers to amount of ceria-zirconia ($Ce_{0.7}Zr_{0.3}O_2$) present in the sample instead of CeO_2. Series 3 differs from the two other series in the amount of precious metal present in the washcoat. The Rh concentration was reduced from 0.71 to 0.35 g/L for the two samples, and the Pt concentration varied at 1.77 g/L (50 g/ft^3) and 3.53 g/L (100 g/ft^3). The two samples in series 3 are designated by the amount of platinum present: Pt-50 and Pt-100. The CeO_2 loading was held constant for both samples at 50 g/L. The total washcoat loading for all of the samples was 260 g/L and was held constant by adjusting the amount of balance Al_2O_3 present.

2.4. Monolith catalyst sulfation and desulfation

1.75 cm × 2.54 cm ($d \times l$) sample cores were drilled from the monolith samples. A small hole was drilled in the center of each core so that a K-type thermocouple could be inserted to measure the temperature of the gas stream at the front face of the sample. The catalyst cores were contained in a vertical quartz tube reactor (1 in. outer diameter) heated by a Lindberg Blue electric furnace. Prior to sulfation/desulfation experiments, samples were degreened (stabilized) by heating at 800 °C for 3 h in a slightly rich gas. The composition of the feed gas is listed in Table 3. The overall flow rate was 3 L/min, resulting in a GHSV of 30,000 h^{-1}.

Monolith samples were sulfated at 350 °C for 16 h using the gas stream shown in Table 3. The gas stream alternated between 1 min lean periods to 1 min rich periods (1/1 cycles).

The length of the rich period was chosen to ensure that the trap was completely purged of NO_x before the next lean cycle. NO_x concentrations were measured using a heated chemiluminescence detector (Beckman Industrial Model 951 NO/NO_x analyzer). The data were used to calculate the NO_x storage efficiency at every hour from the start of sulfation to the end of the 16 h period.

Sample desulfation was performed at one of the following temperatures: 650, 675, 700, 725, or 750 °C. To begin the desulfation, the sample was ramped to the desired desulfation temperature. During the ramp, 1 min lean/1 min rich alternating cycles were used until the temperature reached 580 °C, at which point the feed was switched to the lean gas mixture to prevent desorption of the sulfur stored on the monolith sample before the desulfation temperature was reached. Once the desulfation temperature was obtained, the conditions were switched to rich and the temperature was held constant for 5 min before cooling to 580 °C under lean conditions. At this point, the gas composition was switched from lean to alternating 5 min lean, 3 min rich cycles until the sample reached 350 °C. At 350 °C data were taken from three 5/3 cycles and then five 1/1 cycles, corresponding to "steady state" cycling conditions (i.e., reproducibly periodic). The schedule of heating to the desulfation temperature, cooling to 350 °C, and then evaluating the catalyst during the 5/3 and 1/1 cycles was repeated three times. After the third time the SO_2 was turned off and the sample was heated to 750 °C under rich conditions for 10 min using the method described above. This part of the cycle is referred to as the clean-off. After the clean-off, the sample was evaluated at 350 °C as before using 5/3 and 1/1 cycles. At this point the sample was ready to be sulfated again so the catalyst could be studied at another desulfation temperature. It should be noted that the data from the 1/1 cycles are very similar to the 5/3 cycles in both the storage efficiency values obtained and the resulting trends, and consequently, the 1/1 cycle data are not discussed in this paper.

2.5. Measurement of total sulfur release during desulfation

In these experiments, the same lean and rich gas mixtures were used as for the sulfation–desulfation experiments described in Section 2.4 with the exception that in order to expedite catalyst sulfation, the samples were sulfated with 90 ppm SO_2 at 350 °C (for 1 h under lean conditions; see Table 4). After sulfation, the SO_2 was shut off, and the sample was heated to the desired desulfation temperature under lean conditions to avoid any loss of SO_2. Once the desulfation temperature was reached, the feed was switched to the rich gas mixture containing CO and H_2 for 10 min. Each desulfation ended with heating the sample to 750 °C under lean conditions and then switching to rich conditions for 10 min. Again, the period at 750 °C is referred to a clean-off and was performed to remove as much sulfur as possible before the next sulfation experiment and to confirm the total amount of sulfur originally stored on the catalyst. This allowed the calculation of the fractional sulfur release as a function of temperature by comparing the amount of the total sulfur released at the desulfation temperature to the amount of sulfur released during the clean-off period. The gas composition at the catalyst outlet was continuously monitored during desulfation using a V&F Systems, Inc. chemical ionization mass spectrometer (CI-MS) equipped with three ion sources of different energies. Mercury is the low energy source and is used to detect H_2S. Xenon is the medium source and is used to detect SO_2 and COS. Krypton is the high energy source and was not used in this study. From the concentrations of the sulfur species evolved, the data were integrated to calculate how much of each species was released during desulfation and during the clean-off. The fraction of total sulfur released was used to compare and evaluate the performance of the monolith catalysts.

Table 3
Feed gas composition during determination of NO_x storage efficiency.

Component	Lean	Rich
CO_2	10%	10%
H_2O	10%	10%
NO_x	500 ppm	500 ppm
SO_2	9 ppm	9 ppm
O_2	5%	0
CO	0	1.20%
H_2	0	0.40%
N_2	Balance	Balance

Table 4
Feed gas composition during determination of fraction of sulfur released/stored.

Component	Lean	Rich
CO_2	10%	10%
H_2O	10%	10%
NO_x	500 ppm	500 ppm
SO_2	90 ppm	90 ppm
O_2	5%	0
CO	0	1.20%
H_2	0	0.40%
N_2	Balance	Balance

3. Results and discussion

3.1. Powder model catalysts

3.1.1. Temperature-programmed reduction

Four model catalysts were examined in this study, comprising Pt/Al_2O_3, Pt/CeO_2, PBA, and PBAC. The Pt/Al_2O_3 and Pt/CeO_2 samples were used as references to distinguish between release events from alumina, ceria, and barium sites. Prior to TPR, the samples were sulfated to loadings of 1, 2.5, and 7.5 g sulfur adsorbed per liter equivalent of monolithic catalyst (assuming a typical monolith washcoat loading of 260 g/L). A typical release of the sulfur species observed during TPR is shown in Fig. 1 for Pt/Al_2O_3. The first species seen is SO_2 which is then followed by H_2S. COS is also seen when SO_2 release begins, but unlike the concentration of SO_2, which decreases for the remainder of the TPR, the concentration of COS continues to increase until about 750 °C. Given that H_2S is the main product during the TPR experiment, in the following TPR plots only the H_2S release events are shown. Table 5 and Fig. 2 summarize the results of the TPR experiments performed using Pt/Al_2O_3. At a loading equivalent to 1 g S/L, the H_2S release began at 369 °C, peaked at 399 °C, and ended at 627 °C. As the sulfur loading was increased to 2.5 g S/L equivalent and then 7.5 g S/L, also shown in Fig. 2, the release of H_2S began at temperatures slightly lower than at the 1 g S/L loading (358 and 356 °C, respectively). The reason for the lowering of the first release temperature as the sulfur loading was increased is not totally clear; however, it is probably due to the fact that at low loadings sulfur is stored at the strongest adsorption sites (e.g., the most basic). As the loading is increased, these sites are filled and sulfur is increasingly stored at sites where it is more weakly adsorbed. The maximum for this release event occurred at 368 °C for the 2.5 g S/L loading and 381 °C for the 7.5 g S/L sample. As the sulfur loadings increased so did the amount of sulfur released during TPR. In all three samples, the majority of the sulfur released was seen as H_2S, its release peaking below 400 °C. This result is broadly comparable with results reported in the literature. Wei et al. reported that peak H_2S evolution from Pt/Al_2O_3 occurred at 410 [31], while Elbouazzaoui et al. reported H_2S release from Pt/Al_2O_3 starting at 300 °C and peaking at 450 °C [11].

TPR results for Pt/CeO_2 are shown in Table 5 and Fig. 3. For the sulfur loadings of 1.0 g S/L, 2.5 g S/L and 7.5 g S/L, H_2S evolution

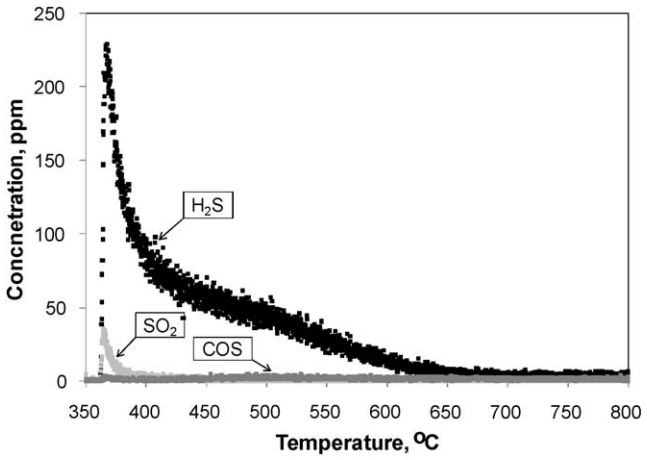

Fig. 1. Sulfur species released from Pt/Al_2O_3 sulfated to 2.5 g sulfur/L of catalyst equivalent during TPR. Gas composition: 2% H_2, 5% CO_2 and 5% H_2O, balance Ar, GHSV = 30,000 h^{-1}.

commenced at 459, 415, and 423 °C, respectively, with the corresponding peak H_2S releases at 518, 463, and 451 °C. These values compare well with the temperatures reported by Ji et al. (450 °C) [17], Bazin et al. (400–500 °C) [32,33] and Waqif et al. (480–550 °C) [34] for sulfate reduction and concomitant sulfur release from sulfated ceria. Similar to the Pt/Al_2O_3 samples, the total amount of sulfur released from Pt/CeO_2 during TPR increased with increasing sample exposure to SO_2, while for all three sulfur loadings H_2S was the main species released by mass. In addition, there were indications of a possible minor secondary H_2S release event centered at approximately 750 °C (see inset, Fig. 3). However, the magnitude of this event was such that it is hard to distinguish it from analytical noise, and consequently we have chosen not to include it in Table 5.

Turning to catalyst PBA, for the 1 g S/L loading (Table 5 and Fig. 4), SO_2 release was observed at 400 °C, followed by the release of H_2S that peaked at 477 °C. The evolution of these sulfur species can be assigned to sulfur release from alumina as seen for the Pt/Al_2O_3 reference sample. A second release event started at about 573 °C and continued until 800 °C with the peak H_2S concentration occurring at 729 °C. This is associated with Pt promoted

Table 5
Relative amounts of H_2S released from different storage components during temperature-programmed reduction.[a]

Equivalent S loading, g/L			1		2.5		7.5	
Sample	Storage component	Type	% H_2S	Peak temperature, °C	% H_2S	Peak temperature, °C	% H_2S	Peak temperature, °C
Pt/Al_2O_3	Al_2O_3	Surface	80	399	100	368	100	381
		Bulk	20	797	N/D[b]	–	N/D	–
Pt/CeO_2	CeO_2	Surface	100	518	100	463	100	451
PBA	Al_2O_3	Surface	9	477	11	433	35	384
	BaO	Surface	91	729	89	706	48	682
		Bulk	N/D	–	N/D	–	17	773
PBAC	Al_2O_3	Surface	N/D	–	N/D	–	1	382
		Bulk	N/D	–	N/D	–	–	–
	CeO_2	Surface	35	465	43	462	62	451
		Bulk	–	–	–	–	–	–
	BaO	Surface	65	737	57	748	27	682
		Bulk	N/D	–	N/D	–	10	781
Pt/Al_2O_3:BaO/Al_2O_3	Al_2O_3	Surface	46	378	54	367	–	–
		Bulk	N/D	–	N/D	–	–	–
	BaO	Surface	19	748	21	735	–	–
		Bulk	34	791	25	766	–	–

[a] Rich phase for TPR: 2% H_2, 5% CO_2, 5% H_2O, Ar balance, GHSV = 30,000 h^{-1}.
[b] N/D: not detectable by CI-MS during the experiment.

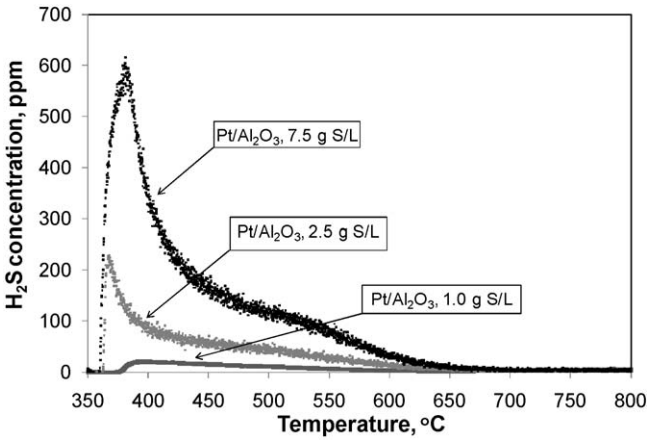

Fig. 2. Comparison of H_2S released from Pt/Al_2O_3 sulfated to 1.0, 2.5, and 7.5 g sulfur/L of catalyst during TPR. Gas composition as for Fig. 1.

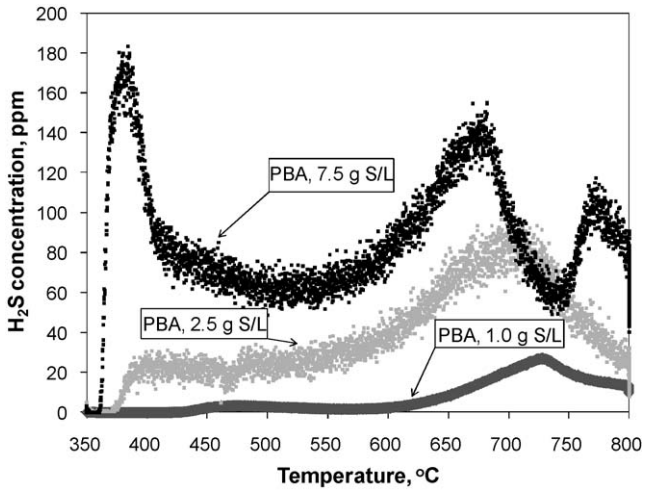

Fig. 4. Comparison of H_2S released from PBA sulfated to 1.0, 2.5, and 7.5 g sulfur/L of catalyst during TPR. Gas composition as for Fig. 1.

decomposition of $BaSO_4$ in accordance with previous reports of the temperature maxima for $BaSO_4$ decomposition in sulfated $Pt/Ba/Al_2O_3$ samples by Elbouazzaoui (650 °C for surface $BaSO_4$ and 750 °C for bulk $BaSO_4$), Ji (650 °C), and Stakheev (600–610 °C for surface $BaSO_4$ and ~700–720 °C for bulk $BaSO_4$) [4,17,35]. With the increase of the sulfur loading to 2.5 and 7.5 g S/L (also shown in Fig. 4), the onset of sulfur release began at lower temperatures (366 and 355 °C, respectively), this event again being ascribed to sulfur release from Al_2O_3. The second release event for both loadings took place at 550 °C and in the case of the 2.5 g S/L sample reached a maximum concentration at 706 °C, a slightly lower value than for the sample sulfated to 1 g S/L. This result is consistent with the increase in sulfur loading and shift to a lower release temperature observed for the other samples. In the case of the 7.5 g S/L sample, a double peak was observed at high temperature. The first maximum of this double peak occurred at 682 °C, and the second occurred at 773 °C. The first of the maxima can be assigned to the release of sulfur stored as surface $BaSO_4$, while the second can be attributed to sulfur stored as bulk $BaSO_4$.

Several authors have made similar observations that temperatures above 700 °C are required for the decomposition of bulk $BaSO_4$ [4,11,35]. Seldmair et al. reported that during sulfation surface sulfates can undergo migration into the support material to become bulk sulfates [36]. Elbouazzaoui et al. concluded that peaks corresponding to surface and bulk $BaSO_4$ were present in the TPR profile of a sulfated $Pt/BaO/Al_2O_3$ catalyst [4,11]. These workers postulated that Pt promotes the reduction of surface $BaSO_4$ deposited in the vicinity of Pt but has no effect on $BaSO_4$ located far from the metal sites. Using Raman spectroscopy, Wei et al. concluded that $BaSO_4$ close to Pt particles has a small crystallite size (< 3 nm) and is reduced at moderate temperatures (~650 °C). On the other hand, bulk sulfate has a larger crystallite size (> 10 nm) and is reducible only at high temperatures (~750 °C) [31]. Stakheev et al. also proposed that the presence of two peaks is due to surface and bulk barium sulfates or to $BaSO_4$ located close to and far away from Pt particles [35].

Based on the results from the two reference samples and catalyst PBA, the effects of ceria addition to PBA can be demonstrated. Looking at the TPR result for the PBAC sample loaded to 1 g S/L (Fig. 5), two desorption maxima occur at 465 and 737 °C. The first release event can be assigned to release from ceria as seen with the Pt/CeO_2 sample, while the second corresponds to the release of sulfur from $BaSO_4$, as seen with PBA. Comparing the PBAC and PBA samples at 1 g S/L, Table 5, the amount of H_2S released from Ba sites reflects the presence of ceria with a difference of 26% less H_2S released from the Ba in PBAC compared

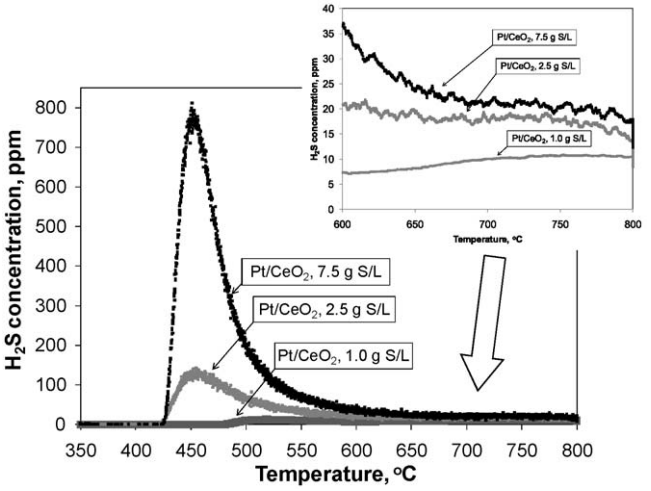

Fig. 3. Comparison of H_2S released from Pt/CeO_2 sulfated to 1.0, 2.5, and 7.5 g sulfur/L of catalyst during TPR. Gas composition as for Fig. 1.

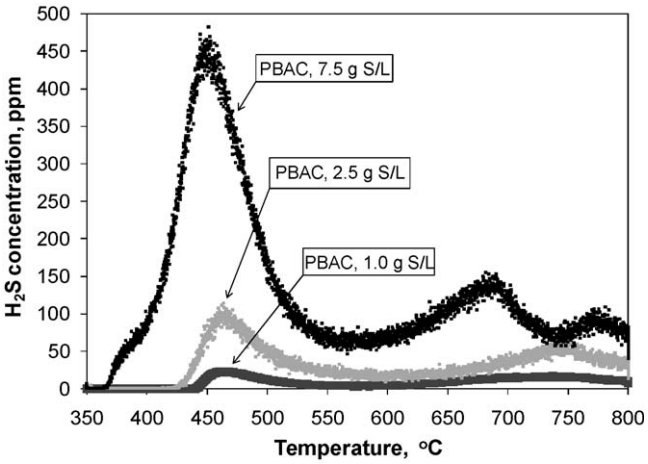

Fig. 5. Comparison of H_2S released from PBAC sulfated to 1.0, 2.5, and 7.5 g sulfur/L of catalyst during TPR. Gas composition as for Fig. 1.

to PBA. Comparing the release from the Al sites in PBA to the Ce sites in PBAC, a 26% difference is again seen in the amount of H_2S evolved. The release of sulfur species from the Ce phases in PBAC demonstrates the additional storage provided by the Ce sites. As seen in Fig. 5, when the loadings were increased from 1 to 2.5 to 7.5 g S/L, the height of the peak from the release of CeO_2 sites increased faster than the peak from the Ba sites. This increase is also reflected in Table 5, where the amount of H_2S released from the Ce sites in PBAC increased from 35% of the total for 1 g S/L loading to 43% for 2.5 g S/L and 62% for 7.5 g S/L. This implies that sulfur was preferentially stored at the CeO_2 sites as opposed to the BaO sites as the loading increased.

3.1.2. Effect of platinum location on desulfation efficiency

In order to demonstrate the influence of Pt location (with respect to the Ba sites) on LNT desulfation, a sample was prepared in which the Pt and Ba phases were separated. This was done by physically mixing 1 wt.% Pt/Al_2O_3 and 20 wt.% BaO/Al_2O_3 powders in a 1:1 weight ratio. As shown in Table 5 and Fig. 6, during TPR the physical mixture displays several H_2S release events. For the sample loaded to 1 g S/L, the first release of H_2S is seen at 356 °C and extends up to 580 °C, with a maximum at 378 °C. The second release begins at 580 °C, peaks at 748 °C and extends up to 752 °C, and the third begins at 752 °C and continues until the end of the TPR experiment at 800 °C, with a maximum at 791 °C. As the sulfur loading is increased to 2.5 g S/L, these maxima are slightly shifted towards lower temperature, as typically observed for the other catalyst samples discussed above.

Comparing the results for the physical mixture and sample PBA, although both samples release about the same amount of sulfur at the 1 g/L S loading (and correspondingly more at the 2.5 g/L loading), several significant differences are observed. First, sulfur release in the range 350–500 °C is observed to occur at lower temperatures and in relatively greater amounts for the physical mixture than for PBA. The release in this temperature range is consistent with the decomposition of sulfate on alumina [11,31], while the releases seen from both samples at the higher temperatures (>580 °C) can be assigned to the decomposition of $BaSO_4$ [4,11,35]. Second, whereas PBA shows a single H_2S release event corresponding to the decomposition of surface $BaSO_4$, the physical mixture shows a double peak corresponding to H_2S release from both surface and bulk $BaSO_4$. Third, the maxima for H_2S release from surface $BaSO_4$ are shifted by between ~20 and 40 °C to higher temperature for the physical mixture as compared to PBA (the exact value being dependent on the sulfur loading). We note that a similar observation has been reported by Wei et al. during related TPR experiments [31]: for a physical mixture of Pt, Rh/Al_2O_3 and BaO/Al_2O_3, the high temperature $BaSO_4$ release maximum occurred at a temperature that was 60 °C higher than for the corresponding peak observed for an impregnated sample containing $BaO/Pt, Rh/Al_2O_3$.

From the foregoing it is apparent that in PBA most of the sulfur is stored on surface BaO sites, whereas in the physical mixture sulfur is stored on both Al_2O_3 and BaO sites. Sulfur storage on the Al_2O_3 sites can be attributed to spillover of SO_3 from Pt to the Al_2O_3 support during sulfation. More significantly, the fact that the desulfation temperature of the Ba storage component is shifted towards higher temperature for the physical mixture relative to PBA is consistent with the idea that the decomposition of surface $BaSO_4$ is facilitated by adsorbed H atoms which spill over from the Pt sites onto the sulfated Ba phase. Physical separation of the Pt and Ba phases appears to inhibit this process, with the consequence that the surface $BaSO_4$ behaves more like bulk $BaSO_4$ with respect to its desulfation properties. We note that somewhat analogous findings have been reported for nitrate decomposition on physical mixtures of Pt/Al_2O_3 and BaO/Al_2O_3 [37]: in the absence of hydrogen spillover from Pt to the Ba phase, considerably higher temperatures are required to achieve nitrate decomposition than is usual for $Pt/BaO/Al_2O_3$ catalysts.

3.2. Monolith catalysts

3.2.1. Effects of sulfur on NO_x storage efficiency and regeneration temperature

In order to shed further light on washcoat component effects in LNT sulfation and desulfation, two experiments were performed using fully formulated monolithic catalysts in which the loadings of the various components (ceria, ceria-zirconia, and precious metals) were systematically varied. In the first experiment, the effect of desulfation at different temperatures on the lean phase NO_x storage efficiency (NSE) during lean-rich cycling was examined. In the second experiment, the ability of the monolith sample to be desulfated under rich conditions was determined by calculating the amount of sulfur released during desulfation.

Considering the results of the first experiment (Fig. 7), sample 30–0, containing 30 g BaO/L but no ceria, showed the largest decrease in the NSE during the lean period, corresponding to a loss of 60% after sulfation of the sample. Furthermore, the 30–0 sample was not able to achieve its pre-sulfation NSE value at any of the desulfation temperatures from 650 to 750 °C, as shown in Fig. 8.

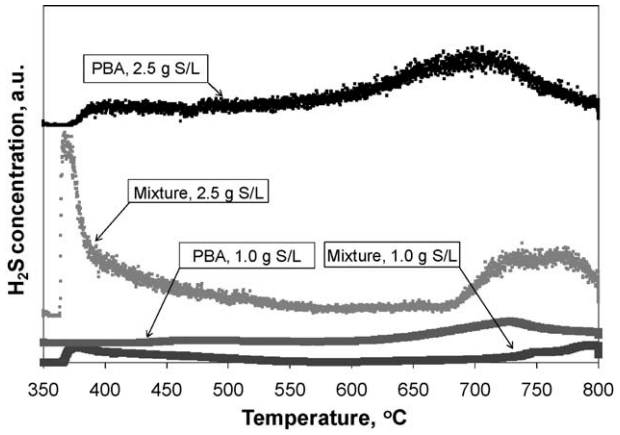

Fig. 6. Comparison of H_2S released from PBA and 1:1 physical mixture of Pt/Al_2O_3 and BaO/Al_2O_3 sulfated to 1.0 and 2.5 g sulfur/L of catalyst during TPR. Gas composition as for Fig. 1. Note that for clarity the plots have been stacked.

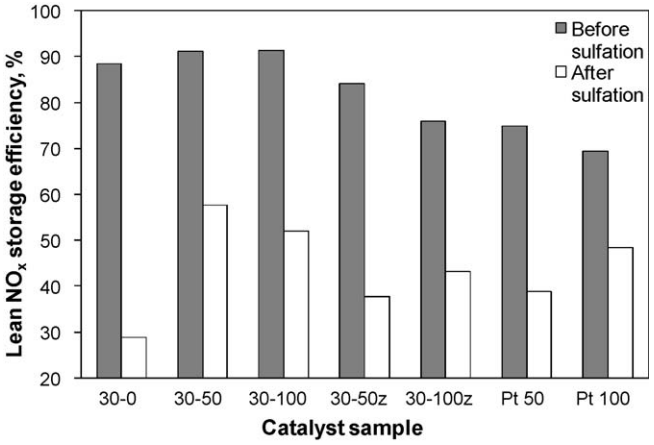

Fig. 7. Comparison of lean NO_x storage efficiency values for fresh and sulfated monolith samples. Samples were sulfated with 9 ppm SO_2 for 16 h at 350 °C under 1 min lean/1 min rich conditions.

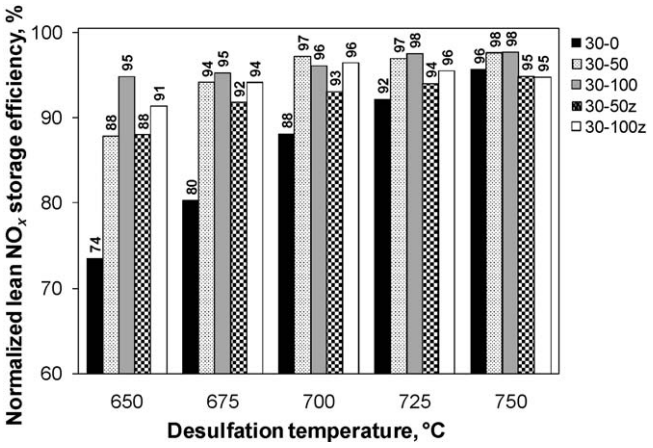

Fig. 8. Comparison of normalized lean NO_x storage efficiency values (NO_x storage efficiency after desulfation divided by the NO_x storage efficiency after clean-off) for samples 30–0, 30–50, 30–100, 30–50*z*, and 30–100*z*. Desulfation conditions: 1.2% CO, 0.4% H_2, 10% CO_2, 10% H_2O, balance N_2, GHSV = 30,000 h^{-1}.

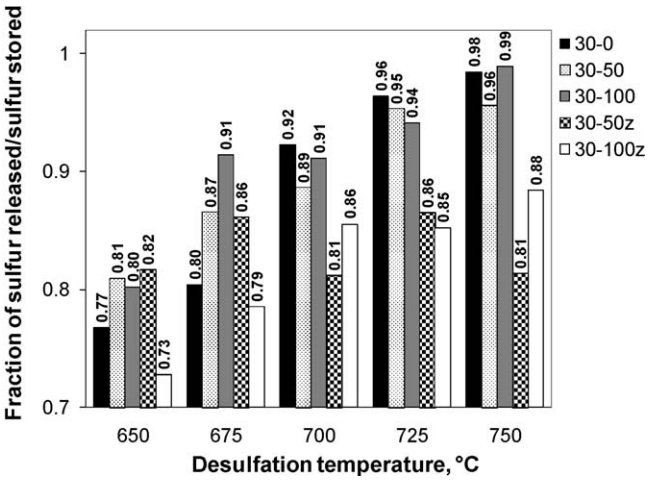

Fig. 9. Comparison of fraction of sulfur released/stored after sulfation with 90 ppm SO_2 for 1 h for samples 30–0, 30–50, 30–100, 30–50*z* and 30–100*z*. Desulfation conditions as for Fig. 8.

The highest value was seen at 750 °C, corresponding to only 96% of the original NSE. Compared to the other catalysts, the NSE of 30–0 showed the greatest dependence on desulfation temperature (difference of greater than 20% over the temperature range). This finding can be explained on the basis of the TPR results presented above for catalyst PBA. Looking at Fig. 4, it is evident that a temperature of less than 750 °C is insufficient to completely desulfate sample 30–0.

Turning to the 30–50 and 30–100 samples containing 50 and 100 g/L of ceria, respectively, the presence of ceria in the monolith results in a higher NSE after sulfation (relative to 30–0) and a clear lowering of the desulfation temperatures required to approach the pre-sulfation NSE values of the catalysts. The NSE values after sulfation for 30–50 and 30–100 are roughly twice the value for 30–0 (Fig. 7). As shown in Fig. 8, sample 30–50 reached 94% of its clean-off NSE value at 675 °C and 97% at 700 °C. Sample 30–100 was even better than 30–50, reaching 95% of its clean-off value at 650 °C. Indeed, in general the NO_x storage efficiency of 30–100 was higher over the entire temperature range used for desulfation than 30–0 or 30–50. The reason for the superior performance of 30–50 and 30–100 over 30–0 can be assigned to the presence of CeO_2 in the sample. As seen for PBAC, CeO_2 can store sulfur, thereby decreasing the extent of bulk $BaSO_4$ formation. Further, the CeO_2 phase can be desulfated at relatively low temperature. An additional factor may be the high water–gas shift (WGS) activity of Pt/CeO_2. Indeed, in previous work we have demonstrated the superior WGS activity of 30–50 and 30–100 relative to 30–0 and the higher intra-catalyst H_2 concentrations that result during rich operation [21].

The effects of CeO_2 addition to the monolith catalysts are further supported by studying the fraction of sulfur released from the stored sulfur. Starting with series 1 (see Fig. 9), the effect of CeO_2 is evidenced by the fact that larger fractions of the stored sulfur are released at lower temperatures (650 and 675 °C) as compared to catalyst 30–0. Indeed, sulfur release at these low temperatures increases with ceria loading. The amount of sulfur released during desulfation for the 30–0 sample is lower than 30–50 or 30–100 until 700 °C and higher. The increased fraction of sulfur released is attributed to the additional SO_x storage sites provided by the ceria present in the sample, which as shown by the TPR results presented in Section 3.1.1 above, releases H_2S and SO_2 at significantly lower temperatures than the BaO phase.

In addition to the ceria-containing samples, two samples were examined that contained CeO_2–ZrO_2 so that the effects of CeO_2 and CeO_2–ZrO_2 could be compared. Both samples contained 30 g/L of BaO, as for the series discussed above; the full compositions are given in Table 2 (series 2). The results obtained for this series are also shown in Figs. 7 and 8. While the fresh NO_x storage efficiency value for 30–50*z* was only 7% lower than the value for 30–50 (84% vs. 91%), the measured value for 30–50*z* after sulfation was 20% lower: in absolute terms, the sample 30–50 lost 34% of its NO_x storage efficiency and the 30–50*z* lost 47%. Comparing samples 30–100 and 30–100*z*, the difference in the fresh NSE values was slightly larger (91% for 30–100 vs. 76% for 30–100*z*). However, the difference in the NSE values after sulfation for 30–100 and 30–100*z* was only 9%. Looking at the NSE values after desulfation for these four samples (Fig. 8), the differences were less than 7% at 650 °C and less than 4% over the remaining temperature range.

Data pertaining to the sulfur release during desulfation supports the observation that the catalysts containing CeO_2–ZrO_2 display inferior desulfation characteristics as compared to their La-stabilized CeO_2-containing analogs (see Fig. 9). This may be attributed to the less basic nature of the CeO_2–ZrO_2 (relative to CeO_2), which may lower the ability of CeO_2–ZrO_2 to store sulfur and hence result in comparatively more severe sulfation of the Ba phase. Indeed, Rohart et al. have reported that the basicity of Ce-mixed oxides affects their SO_x storage capacity [38], sulfate adsorption being higher on ceria-rich oxides than on zirconia-rich oxides. Also relevant in this context are the results of a recent study by Bazin et al. [33], who found that the addition of zirconia into ceria limits sulfation in the bulk of the oxide, thereby limiting the total sulfur uptake. The same authors also report that zirconia addition raises the required desulfation temperature slightly; for example, weight loss maxima of 733 and 753 K were observed during hydrogen reduction of sulfated CeO_2 and $Ce_{0.63}Zr_{0.37}O_2$, respectively. Note that the surface areas of the La-stablilized CeO_2 and CeO_2–ZrO_2 used in the monolithic catalysts in the present study were very similar (119 and 114 m^2/g, respectively), hence surface area should not be a factor with respect to their differing sulfation–desulfation behavior.

Finally, we note that ease of catalyst desulfation (as reflected in the fraction of sulfur released/sulfur stored) holds implications for long term catalyst use, given that the catalyst is subjected to repeated sulfation–desulfation cycles over the course of its useful life. For additives or specific compositions which negatively affect sulfur release from the catalyst, there is a greater tendency to accumulate residual sulfur during repeated sulfur/desulfation events, eventually leading to reduced NO_x storage efficiency. In an

accompanying paper in this journal [39] we describe the results of accelerated aging experiments performed on catalysts 30–0, 30–50, 30–100 and 30–100*z* in which repetitive sulfation/desulfation cycles were performed, and we correlate the residual sulfur contents of the catalysts with their composition. The resulting data confirm that ceria-containing catalysts exhibit superior sulfation and desulfation characteristics as compared to their non-ceria analog; more particularly, the ability of ceria to trap sulfur results in decreased sulfur accumulation on the main Ba NO_x storage component. In addition, while the results presented above suggest that catalyst 30–100*z* should perform less well in this respect than 30–100, the NO_x conversion of 30–100*z* after aging is in fact slightly better than that of 30–100 [39]. The reason for this is not entirely clear, although it may be a consequence of the superior stability of the $Ce_{0.7}Zr_{0.3}O_2$ mixed oxide with respect to thermally induced sintering as compared to La-stabilized CeO_2.

3.2.2. Effect of precious metal loading on NO_x storage efficiency and regeneration temperature

In the last group of catalysts (Series 3, Table 2), the amount of Pt was varied and the amount of Rh was halved. The two samples examined corresponded to Pt-50, containing 50 g/ft^3 (1.77 g/L) Pt and 10 g/ft^3 (0.35 g/L) Rh, and Pt-100, containing 100 g/ft^3 (3.53 g/L) Pt and 10 g/ft^3 (0.35 g/L) Rh. The BaO and CeO_2 loadings were fixed at 30 g/L and 50 g/L, respectively (i.e., as for catalyst 30–50). Looking at the comparison of NO_x storage efficiency values for fresh and sulfated monolith samples (Fig. 7), it is evident that the 30–50 sample, with double the amount of Rh, is less susceptible to poisoning than the Pt-50 or Pt-100 samples. Furthermore, as shown in Fig. 10, clear trends emerge when considering the NSE of the catalysts subjected to desulfation in the range 700–750 °C. Specifically, the NSE of sample 30–50 is found to be slightly higher than that of Pt-100 after desulfation at temperatures of 700 °C and above, a finding which can be ascribed to the lower Rh loading in the latter sample. These results are consistent with the reports of Amberntsson et al. [40,41], who for Ba-based LNTs containing either Pt, Rh or Pt + Rh observed that the recovery of NO_x storage capacity after desulfation in H_2 at 750 °C was complete only for the samples containing both Pt and Rh. This was attributed to the fact that Rh is more easily sulfur-regenerated than Pt [40]. Furthermore, it was found that Rh suffered from severe deactivation with respect to its NO oxidation function under SO_2 exposure but retained high NO_x reduction activity under rich conditions; in contrast, the opposite behavior was observed for Pt. Consequently, it was concluded that a combination of Pt and Rh is preferable for minimizing the effects of

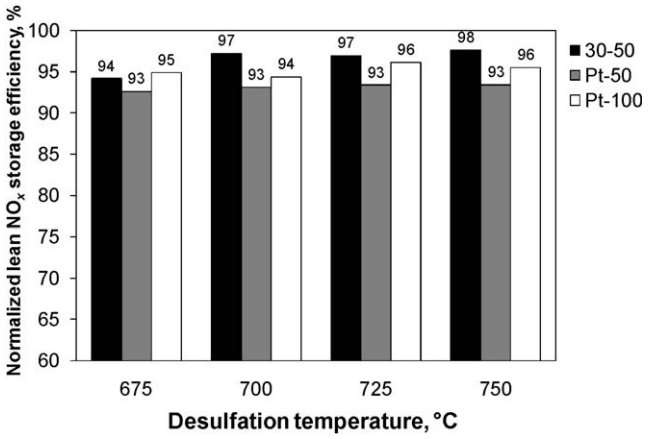

Fig. 10. Comparison of normalized lean NO_x storage efficiency values (NO_x storage efficiency after desulfation divided by the NO_x storage efficiency after clean-off) for samples 30–50, Pt-50, Pt-100. Desulfation conditions as for Fig. 8.

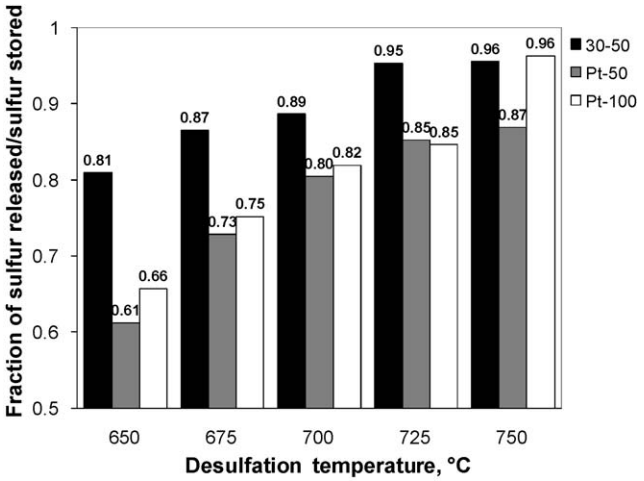

Fig. 11. Comparison of fraction of sulfur released/stored after sulfation with 90 ppm SO_2 for 1 h for samples 30–50, Pt-50 and Pt-100. Desulfation conditions as for Fig. 8.

sulfur deactivation [40,41]. In the case of Pt, it is known that under rich conditions Pt sulfides and/or elemental sulfur can form which block the Pt sites with respect to the adsorption of reductants [36,42]. From this it follows that desulfation should proceed most efficiently when a high concentration of Rh is present, since the Rh will be less susceptible to poisoning by the released sulfur and will enable the continuous adsorption and spillover of reductant molecules onto the sulfated oxides present.

Catalyst Pt-100, in turn, displays higher NSE at each of the desulfation temperatures when compared to catalyst Pt-50, a result which can be directly attributed to the extra Pt present. As a consequence of the additional platinum in Pt-100, the average distance between the Pt sites and the storage components should be decreased as compared to Pt-50 [43]. The effect of the increased proximity of the Pt to the sulfates stored at BaO was demonstrated in the PBA and $Pt/Al_2O_3 + BaO/Al_2O_3$ powders in Section 3.1.2. Specifically, decreasing the Pt–Ba distance can be anticipated to result in more efficient spillover of reductants from the Pt sites and hence, more extensive desulfation. Fig. 11 shows the effects of precious metal loading on the fraction of sulfur released from the samples by comparing the results for the series 3 catalysts to those obtained for 30–50. At almost every temperature, Pt-100 released a greater amount of stored sulfur than Pt-50, consistent with this reasoning.

Overall, in comparing all three of the series of monolith catalysts, the CeO_2 loading is observed to exert a greater influence on catalyst desulfation characteristics than the Pt loading (within the range studied), particularly at temperatures below 700 °C. Correspondingly, the results from the experiments in which sulfur evolution was monitored parallel the results gained from the NO_x storage efficiency experiments. Comparing the three series of catalysts, the catalysts with the highest amounts of CeO_2 or CeO_2–ZrO_2 have the best performance, as measured by the temperature required during desulfation to reach each individual catalyst's clean-off NSE value. A second measure of performance is the resistance to sulfur deactivation in the first place, where again the higher CeO_2 and CeO_2–ZrO_2 containing samples have the best performance. Catalyst 30–100, the sample with the highest amount of CeO_2, showed the best performance in NO_x storage efficiency across all of the desulfation temperatures.

4. Conclusions

The effects of ceria on the sulfation and desulfation characteristics of Ba-based LNT catalysts have been demonstrated using

both powder and fully formulated monolithic catalysts. TPR experiments performed on the powder catalysts showed that each of the oxide phases present (BaO, CeO_2, and Al_2O_3) is able to store sulfur and that they possess distinct behavior in terms of the temperatures at which desulfation occurs. Overall, these findings confirm the idea that ceria can function as a sulfur sink in LNT catalysts, thereby helping to protect the main Ba NO_x storage phase from sulfation.

In addition, the importance of maintaining the Pt and Ba phases in close proximity for efficient LNT desulfation has been demonstrated. It is evident that when Pt and Ba are physically separated, the desulfation temperature of the surface $BaSO_4$ is shifted by 20–40 °C towards higher temperature, i.e., towards the position characteristic of bulk $BaSO_4$. This observation is consistent with the idea that decomposition of surface $BaSO_4$ is facilitated by H ad-atoms which spill over from the Pt sites onto the sulfated Ba phase. Physical separation of the Pt and Ba phases appears to inhibit this process, with the consequence that the surface $BaSO_4$ behaves more like bulk $BaSO_4$ with respect to its desulfation properties. This finding is analogous to the results of nitrate decomposition studied on physical mixtures of Pt/Al_2O_3 and BaO/Al_2O_3 [37].

From the monolith studies, it was found that relative to a sample containing no ceria, samples containing La-stabilized CeO_2 or CeO_2–ZrO_2 showed: (1) a greater resistance to deactivation during sulfation (as reflected by the NO_x storage efficiency) and (2) required lower temperatures to restore the NO_x storage efficiency to its pre-sulfation value. Additionally, the CeO_2-containing catalysts (series 1) released greater fractions of stored sulfur during desulfation. In addition to the ability of ceria to store sulfur and release it at relatively low temperatures under reducing conditions, these results can be attributed to the high water–gas shift activity displayed Pt/CeO_2, which result in increased intra-catalysts concentrations of H_2 under rich conditions. The results also showed that precious metal loadings can significantly impact desulfation efficiency and that both high Rh and Pt loadings are beneficial for catalyst desulfation.

Acknowledgement

This publication was prepared with the support of the U.S. Department of Energy, under Award No. DE-FC26-05NT42631. However, any opinions, findings, conclusions, or recommendations expressed herein are those of the authors and do not necessarily reflect the views of the DOE.

References

[1] J. Theis, J. Ura, C. Goralski, H. Jen, E. Thanasiu, Y. Graves, A. Takami, H. Yamada, S. Miyoshi, SAE Paper No. 2003-01-1160.
[2] V.I. Parvulescu, G. Grange, B. Delmon, Catal. Today 46 (1998) 233.
[3] L. Lietti, P. Forzatti, I. Nova, E. Tronconi, J. Catal. 204 (2001) 175.
[4] S. Elbouazzaoui, E.C. Corbos, X. Courtois, P. Marecot, D. Duprez, Appl. Catal. B 61 (2005) 236.
[5] B. Jang, T. Yeon, H. Han, Y. Park, J. Yie, Catal. Lett. 77 (2001) 21.
[6] D. Kim, Y. Chin, J. Kwak, J. Szanyi, C.H.F. Peden, Catal. Lett. 105 (2005) 259.
[7] M. Casapu, J. Grunwaldt, M. Maciejewski, M. Wittrock, U. Göbel, A. Baiker, Appl. Catal. B 63 (2006) 232.
[8] M. Casapu, J. Grunwaldt, M. Maciejewski, A. Baiker, M. Wittrock, U. Göbel, S. Eckhoff, Top. Catal. 42–43 (2007) 3.
[9] S. Matsumoto, CATTECH 4 (2000) 102.
[10] G. Graham, H. Jen, W. Chun, H. Sun, X. Pan, R. McCabe, Catal. Lett. 93 (2004) 129.
[11] S. Elbouazzaoui, X. Courtois, P. Marecot, D. Duprez, Top. Catal. 30/31 (2004) 493.
[12] N. Fekete, R. Kemmler, D. Voigtländer, B. Krutzsch, E. Zimmer, G. Wenninger, W. Strehlau, J. van den Tilaart, J. Leyrer, E. Lox, W. Müller, SAE Technical Paper Series, 970746, 1997, p. 249
[13] D. Kim, Y. Chin, G. Muntean, A. Yereretz, N. Currier, W. Epling, H. Chen, H. Hess, C.H.F. Peden, Ind. Eng. Chem. Res. 45 (2006) 8815.
[14] M.A. Peralta, V.G. Milt, L.M. Cornaglia, C.A. Querini, J. Catal. 242 (2006) 118.
[15] E. Corbos, X. Courtois, N. Bion, P. Marecot, D. Duprez, Appl. Catal. B 80 (2008) 62.
[16] J. Kwak, D. Kim, J. Szanyi, C.H.F. Peden, Appl. Catal. B 84 (2008) 545.
[17] Y. Ji, T.J. Topps, M. Crocker, Catal. Lett. 127 (2009) 55.
[18] P. Eastwood, Critical Topics in Exhaust Gas After Treatment, Research Studies Press, Ltd., Baldock, Hertfordshire, England, 2000, 231 pp.
[19] Y. Ji, T.J. Toops, M. Crocker, Catal. Lett. 119 (2007) 257.
[20] K. Adams, G. Graham, Appl. Catal. B 80 (2008) 343.
[21] Y. Ji, J.S. Choi, T.J. Toops, M. Crocker, M. Naseri, Catal. Today 136 (2008) 146.
[22] G. Jacobs, L. Williams, U. Graham, D. Sparks, B. Davis, Appl. Catal. A 252 (2003) 107.
[23] A. Phatak, N. Koryabkina, S. Rai, J.L. Ratts, W. Ruettinger, R.J. Farrauto, G.E. Blau, W.N. Deglass, F.H. Ribeiro, Catal. Today 123 (2007) 224.
[24] S. Poulston, R.R. Rajaram, Catal. Today 81 (2003) 603.
[25] Z. Liu, J. Anderson, J. Catal. 224 (2004) 18.
[26] P. Jozsa, E. Jobson, M. Larsson, Top. Catal. 30/31 (2004) 177–180.
[27] T. Szailer, J. Kwak, D. Kim, J. Hanson, C. Peden, J. Szanyi, J. Catal. 239 (2006) 51.
[28] Y. Ji, T.J. Toops, J.A. Pihl, M. Crocker, Appl. Catal. B 91 (2009) 329.
[29] H. Mahzoul, J. Brilhac, B. Stanmore, Top. Catal. 16/17 (2001) 293.
[30] Z. Liu, J. Anderson, J. Catal. 228 (2004) 243.
[31] X. Wei, X. Liu, M. Deeba, Appl. Catal. B 58 (2005) 41.
[32] P. Bazin, O. Saur, J. Lavalley, G. Blanchard, V. Visciglio, O. Touret, Appl. Catal. B 13 (1997) 265.
[33] P. Bazin, O. Saur, F.C. Meunier, M. Daturi, J.C. Lavalley, A.M. Le Govic, V. Harlé, G. Blanchard, Appl. Catal. B 90 (2009) 368.
[34] M. Waqif, P. Bazin, O. Saur, J. Lavalley, G. Blanchard, O. Touret, Appl. Catal. B 11 (1997) 193.
[35] A. Stakheev, P. Gabrielsson, I. Gekas, N. Teleguina, G. Bragina, N. Tolkachev, G. Baeva, Top. Catal. 42–43 (2007) 143.
[36] C. Sedlmair, K. Seshan, A. Jentys, J.A. Lercher, Catal. Today 75 (2002) 413.
[37] I. Nova, L. Lietti, L. Castoldi, E. Tronconi, P. Forzatti, J. Catal. 239 (2006) 244.
[38] E. Rohart, V. Bellière-Baca, K. Yokota, C. Harlé, Pitois, Top. Catal. 42–43 (2007) 71.
[39] Y. Ji, C. Fisk, V. Easterling, U. Graham, A. Poole, M. Crocker, J.-S. Choi, W. Partridge, K. Wilson, Catal. Today, this issue.
[40] A. Ambertsson, M. Skoglundh, S. Ljungström, E. Fridell, J. Catal. 217 (2003) 253.
[41] A. Ambertsson, E. Fridell, M. Skoglundh, Appl. Catal. B 46 (2003) 429.
[42] C. Sedlmair, K. Seshan, A. Jentys, J.A. Lercher, Res. Chem. Intermed. 29 (2003) 257.
[43] H. Mahzoul, J.F. Brilhac, P. Gilot, Appl. Catal. B 20 (1999) 47.